# Liquid—Liquid Equilibria in Quasi-ternary Systems*

R. KONINGSVELD

*Centraal Laboratorium, DSM, Geleen, The Netherlands*

Received April 1, 1971

The influence of the molecular weight distribution of polymers on liquid—liquid phase relationships is investigated theoretically and illustrated with experimental examples. The polydispersity reveals itself in an identical way irrespective of the kind of system considered. Various types are discussed: solvent—polymer; solvent—polymer 1—polymer 2; polymer 1—polymer 2; solvent—non solvent—polymer. In none of these cases is it permitted to consider the polymeric constituent(s) as a single component. Methods are described to account quantitatively for polydispersity. The efficiency of polymer fractionation is briefly commented upon.

In view of the announced scope of the present Meeting, the title of this contribution might need some explanation. Strictly, in the sense of the thermodynamic definition, a ternary system is built up of three components. However, the systems dealt with at this Conference must, in fact, be defined as consisting of three constituents. One or two of these, or even all three, are polymeric substances which are known to contain many macromolecular components differing at least in chain length. In this paper we argue that the polydispersity should never be ignored, in particular not in thermodynamic phenomena such as phase relationships.

By introducing the term *quasi-ternary* systems we try to indicate that we are not dealing with arbitrary multicomponent systems, but that the components in a constituent are very similar in chemical structure and, in fact, belong to the same homologous series. This implies that copolymers fall outside the scope of the quantitative considerations to be given below. However, the descriptions of the effect of polydispersity will have qualitative validity also for copolymers and branched macromolecules.

The quasi-ternary systems to be discussed comprise either a single solvent and two polydisperse polymers, or two solvents (a good and a poor one) and one polydisperse polymer. Before turning to these, we should first give attention to some quasi-binary systems, that is to say to a mixture of a solvent and a polydisperse polymer. After that, we can proceed to a discussion of the compatibility of two polydisperse polymers. We shall see that the phenomenon of polydispersity manifests itself in quite a similar way also in the more complicated quasi-ternary systems.

## *Solvent—polymer systems*

The meaning of a quasi-binary diagram obtained by plotting liquid—liquid phase relations in the usual two-dimensional graph of cloud-point temperature *vs.* concentration,

* Presented at the meeting on "Thermodynamics of Ternary Polymeric Systems", Bratislava, June 29—30, 1970.

is not at once obvious. An insight can be obtained by considering a ternary system consisting of the solvent $S$ and two polymer homologues $P_1$ and $P_2$ of different molecular weight [1, 2]. Fig. 1 schematically shows the miscibility gap as it may occur in such a mixture at temperatures where one of the binary solvent–polymer systems is partially

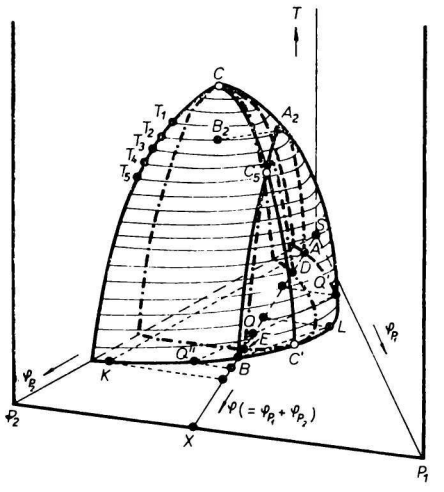


*Fig. 1.* Miscibility gap in a ternary system consisting of a low-molecular-weight solvent $S$ and two macromolecular homologues $P_1$ and $P_2$ of different chain length.
$AA_2C_5B$: cloud-point curve; $CC_5C'$: critical line; $A_2$: precipitation threshold; $DC_5E$: quasi-binary spinodal; $A_2B_2$, $AK$, $BL$ and $Q'Q''$: tie lines (schematical).

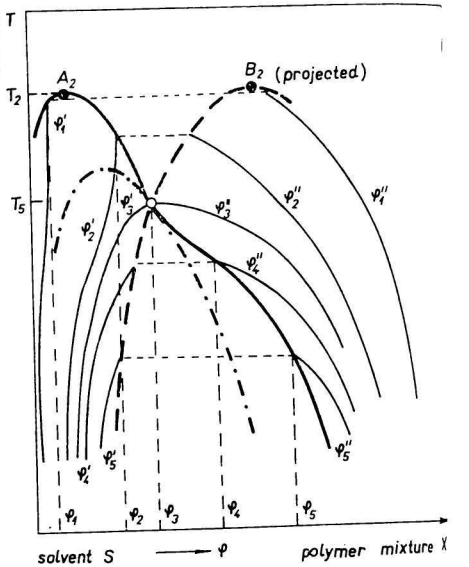


*Fig. 2.* Schematical two-dimensional phase diagram referring to quasi-binary section $TSX$ in Fig. 1.
———— cloud-point curve; — • — • - spinodal; — — — — shadow curve; ———— coexistence curves for various overall polymer concentrations; ○ critical point.

miscible, whereas the other shows complete miscibility ($M_{P1} < M_{P2}$). Located in the $TSP_2$ lateral face is the coexistence curve, well known with partially miscible binary systems, where the consolute state $C$ is found at the extreme of the $T(\varphi_{P2})$ curve ($\varphi_{P2}$ is the volume fraction of $P_2$). Any value of $T < T_c$ corresponds to two cloud points which represent coexisting phases. The location of the stability limit of the system (spinodal) is indicated.

Such a binary two-phase region extends into the ternary temperature-composition prism. Ternary miscibility gaps have been calculated in great detail by *Tompa* [3, 4] on whose diagrams Fig. 1 is based. The coexisting phases are denoted by the end points of the tie lines (*e.g.* $A_2$ and $B_2$, $Q'$ and $Q''$). The locus of these end points is called binodal or coexistence curve. The consolute or critical state is somewhere in the composition triangle ($C'$) and here, as in the binary system, the spinodal has a common tangent with the binodal.

We might consider the binary macromolecular mixture $X$ as a first approximation of a multicomponent polymer. All solutions of $X$ in $S$ can be represented by points on the composition axis $SX$. Evidently, $TSX$ is the plane of drawing for the plot of the cloud points of polymer mixture $X$ in $S$ *vs.* the whole polymer concentration $\varphi$. As a rule, tie lines will be so directed as to fall outside the quasi-binary section $TSX$, meaning that the cloud-point curve does not represent coexisting phases. Further, the extreme $A_2$ of the cloud-point curve, called precipitation threshold by *Tompa* [4, 5], is not a critical point, being shifted as it is towards larger $\varphi(C_5)$ [6], with respect to the threshold.

When a cloud point is reached upon a change in the temperature of a homogeneous solution, a new phase is on the verge of appearing (*e.g.* $K$, $L$, $B_2$). Plotting the compositions of such phases in the two-dimensional graph means projecting them onto $TSX$. The locus of these projections is the coexistence curve of the cloud-point curve, which, escaping direct experimental determination, is briefly referred to as 'shadow curve' [2]. It is obvious that cloud-point and shadow curves must intersect in the critical point.

For a system with an overall composition within the heterogeneous region like $Q$, the two coexisting phase compositions both lie outside $TSX$ ($Q'$ and $Q''$) and can also be projected. The locus of such projections, called coexistence curve, depends on the overall polymer concentration $\varphi$ in that the two branches (dilute and polymer-rich phases) move closer together with increasing $\varphi$. This is easily seen if one considers an increase of $\varphi$ from $A$ to $B$. Summarizing these observations, several of which were made long ago by *Schreinemakers* [7], one is led to the conclusion that the complete two-dimensional phase diagram for a quasi-binary mixture will have the shape shown in Fig. 2. Since the spinodal extends into the prism, $TSX$ intersects the spinodal surface. The quasi-binary spinodal $DC_5E$ has a common tangent with the cloud-point curve at the critical point.

These qualitative considerations on ternary mixtures can be extended to cover truly multicomponent systems, albeit that these cannot be visualized in the same way as above. We have to content ourselves with calculated quasi-binary sections to check whether the above deductions are general. This can be done by using a suitable equation of state for the polymer solution. The simplest equation available is the *Flory–Huggins* lattice expression [8, 9], which gives a good qualitative description of the thermodynamic properties of polymer solutions. Quantitative agreement with experiment can moreover

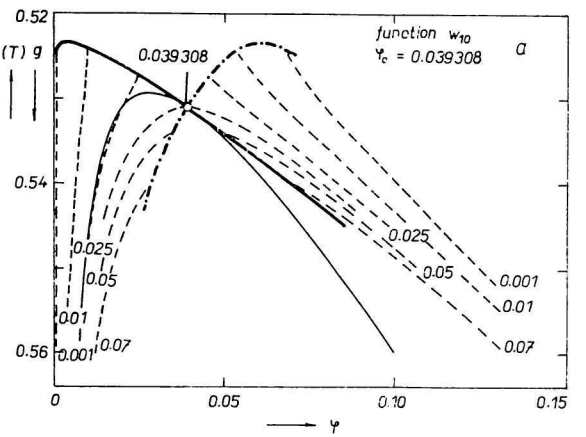


*Fig. 3a.*

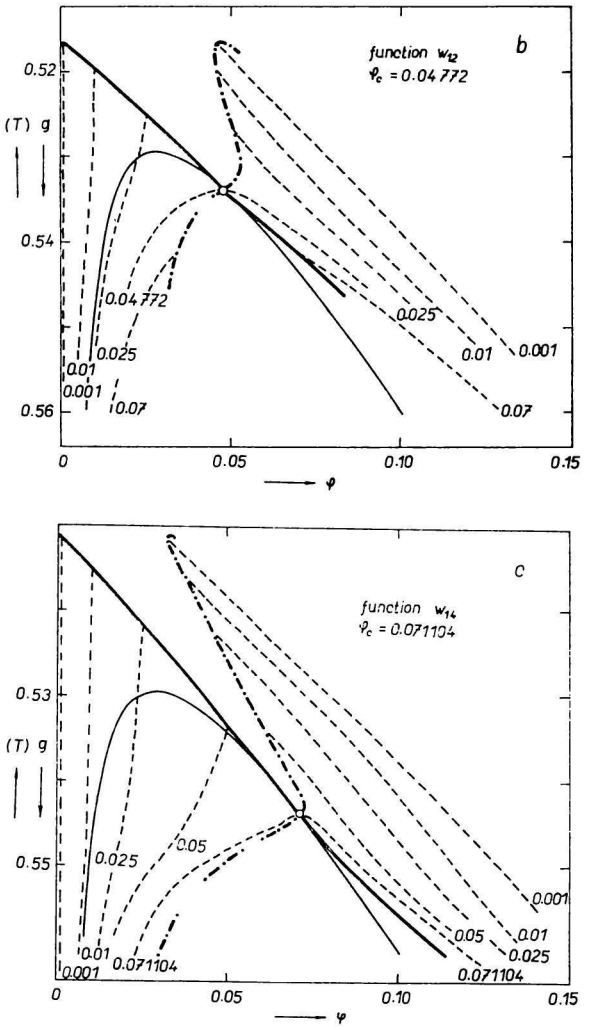


*Fig. 3a—c.* Calculated two-dimensional phase diagrams for three molecular weight distributions (equal in $M_n$ and $M_w$, different in $M_z$; see Fig. 4).
——— cloud-point curves; ———— spinodal; — • — • — shadow curves; — — coexistence curves for various overall polymer concentrations; ○ critical points.

readily be obtained. The following considerations are based upon the Flory—Huggins equation written in the following form

$$\Delta G/RT = \varphi_0 s_0^{-1} \ln \varphi_0 + \sum \varphi_i m_i^{-1} \ln \varphi_i + g(T, \varphi)\, \varphi_0 \varphi, \qquad (1)$$

where $\Delta G$ = free enthalpy (Gibbs free energy) of mixing per mole of lattice sites,
$\varphi_0$ = volume fraction of solvent,
$s_0$ = number of lattice sites occupied by a solvent molecule,

$\varphi_i$ = volume fraction of macromolecular species $i$,
$\varphi = \sum\varphi_i$ = whole polymer volume fraction,
$m_i$ = number of lattice sites occupied by polymer chain $i$ ('chain length'),
$g(T, \varphi)$ = semiempirical free enthalpy correction term,

$R$ and $T$ have the usual meanings.

Phase diagrams can be calculated on the basis of the equilibrium condition that the chemical potential of a component is equal in the two phases. The resulting equations are transcendent and must be solved numerically [1]. To do so, some assumption must be made about the molecular weight distribution of the whole polymer. The polymer composition is brought into account in the second term on the right-hand side of equation (1) since

$$\varphi_i = \varphi\varphi_i^0,$$

where $\varphi_i^0$ stands for the volume fraction of species $i$ in the solvent-free polymer, *i.e.* for the molecular weight distribution.

Fig. 3*a*–*c* shows two-dimensional phase diagrams calculated for three molecular weight distributions having the same weight- and number-average molecular weight $M_w$ and $M_n$, but different z-averages $M_z$. The distribution curves are shown in Fig. 4. The calculation was based upon the assumption that $g$ is independent of $\varphi$. The $g(T)$ function was left unspecified so that $g$, instead of $T$, appears on the ordinate. All features noted in the qualitative ternary example are present also in the multicomponent system (Fig. 3). Further, the shape of the phase diagram depends markedly on the shape of the distribution, becoming distorted as $M_z$ increases. Qualitatively, this corresponds to a shifting of $X$ in Fig. 1, which obviously affects the shape of the quasi-binary section.

There exists experimental evidence showing that these calculated phase diagrams conform to physical reality, first of all in the extensive phase studies on the system polystyrene–cyclohexane by *Rehage et al.* [10, 11] (Fig. 5). Data on the system polyethylene–diphenyl ether offer further support [1] (Fig. 6). They also show that the

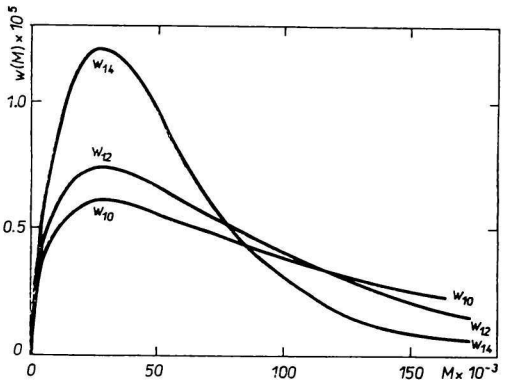


*Fig. 4.* Molecular weight distributions used in the calculation of Fig. 3.
$M_w = 131{,}700$, $M_w/M_n = 5$.
$w_{10} : M_z/M_w = 2$; $w_{12} : M_z/M_w = 3$; $w_{14} : M_z/M_w = 7$.

depression in the cloud-point curve at the critical point calculated for distributions $w_{12}$ and $w_{14}$ may actually occur, and, furthermore, that a shadow curve may bend backwards after having passed the critical point.

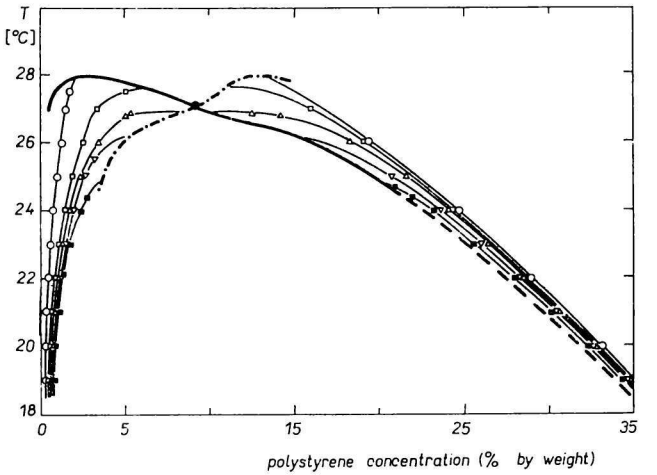


*Fig. 5.* Experimental two-dimensional phase diagram for the quasi-binary system cyclohexane—polystyrene. Data from *Rehage et al.* [10, 11].
——— cloud-point curve; — • — • — shadow curve; coexistence curves for various overall polystyrene concentrations (○ 2%; □ 6%; △ 10%; ▽ 15%; ■ 20% w/w); ● critical point found with the phase-volume method.

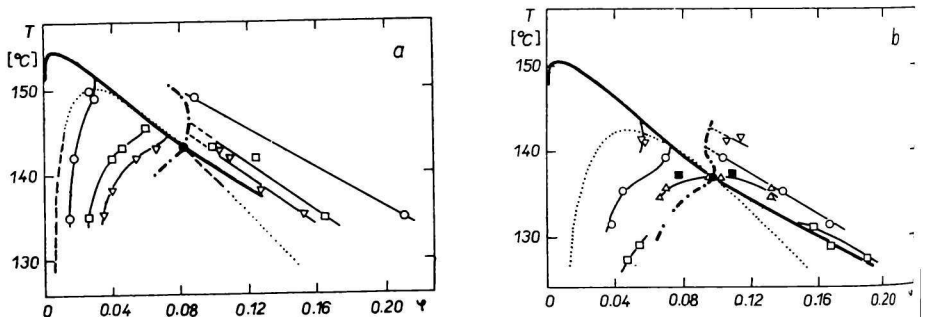


*Fig. 6a, b.* Experimental two-dimensional phase diagrams for two quasi-binary diphenyl ether—polyethylene systems [1].
——— cloud-point curves; — — — — spinodals; — • — • — shadow curves; ——— coexistence curves; ● critical points.
The samples differ in molecular weight distribution.
*a*) Sample L 30-0-7: ○ $\varphi = 0.0309$; □ $\varphi = 0.0612$; ▽ $\varphi = 0.0734$.
*b*) Sample L 30-5-1: ▽ $\varphi = 0.0563$; ○ $\varphi = 0.0733$; ■ $\varphi = 0.0854$; △ $\varphi = 0.0973$ (the critical concentration); □ $\varphi = 0.1445$.

The spinodal and the critical point can be calculated by equating to zero the second and third derivatives of $\Delta G$ with respect to polymer concentration, with allowance being made for polydispersity. *Gibbs* formulated the stability and critical conditions for multicomponent systems [12]. For the spinodal we have (at constant pressure and temperature)

$$J_{sp} = |\partial^2 \Delta G/\partial\varphi_i \partial\varphi_j| = 0 \tag{2}$$

the consolute state being defined by

$$J_{cr} = \begin{vmatrix} \partial J_{sp}/\partial\varphi_1 & \partial J_{sp}/\partial\varphi_2 \\ \partial \Delta G/\partial\varphi_1\partial\varphi_2 & \partial^2 \Delta G/\partial\varphi_2^2 \end{vmatrix} = 0 \tag{3}$$

where $\varphi_i$ and $\varphi_j$ stand for all independent concentration variables (*e.g.* the volume fractions of all polymer components).

Applied to equation (*1*) equations (*2*) and (*3*) yield

$$-(\partial^2\psi/\partial\varphi^2)_{p,T} = 1/(1-\varphi)\, s_0 + 1/\varphi m_w, \tag{2a}$$
(spinodal)

$$-(\partial^3\psi/\partial\varphi^3)_{p,T} = 1/(1-\varphi_c)^2\, s_0 - m_z/m_w^2\varphi_c^2, \tag{3a}$$
(critical point)

where $\psi = g(T, \varphi)\ \varphi_0\varphi$, and $\varphi_c$ is the critical volume fraction of the whole polymer. Consequently, in systems obeying equation (*1*) the detailed shape of the molecular weight distribution does not enter the expressions for the stability limit and critical state. Only the weight- and z-average chain lengths $m_w$ and $m_z$ play a role. This is very fortunate because unlike the distributions, which are difficult to determine with reasonable accuracy, averages like $M_w$ and $M_z$ are readily accessible. The spinodals in Figs. 3*a*–*c* are identical (the distributions are equal in $M_w$) and the critical points move to higher $\varphi$ according as $M_z$ increases [6, 13].

With the right-hand sides of equations (*2a*) and (*3a*) containing measurable quantities,

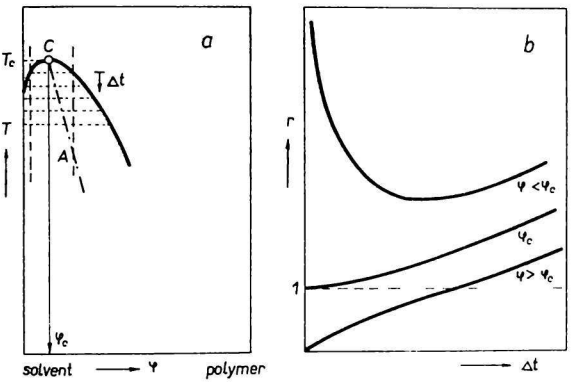


*Fig. 7a, b.* Phase-volume method for locating the critical point. $r = V'/V''$ (volumes dilute and polymer-rich phases).

establishment of consolute states for a series of samples differing in $M_z$ and $M_w$ should allow determination of the interaction function $\psi$. Elsewhere, it has been shown that this method, in fact, offers a very accurate key to the interaction parameter $g$ [14]. In addition to $M_w$ and $M_z$, the location of $\varphi_c$ on the right-hand branch of the cloud-point

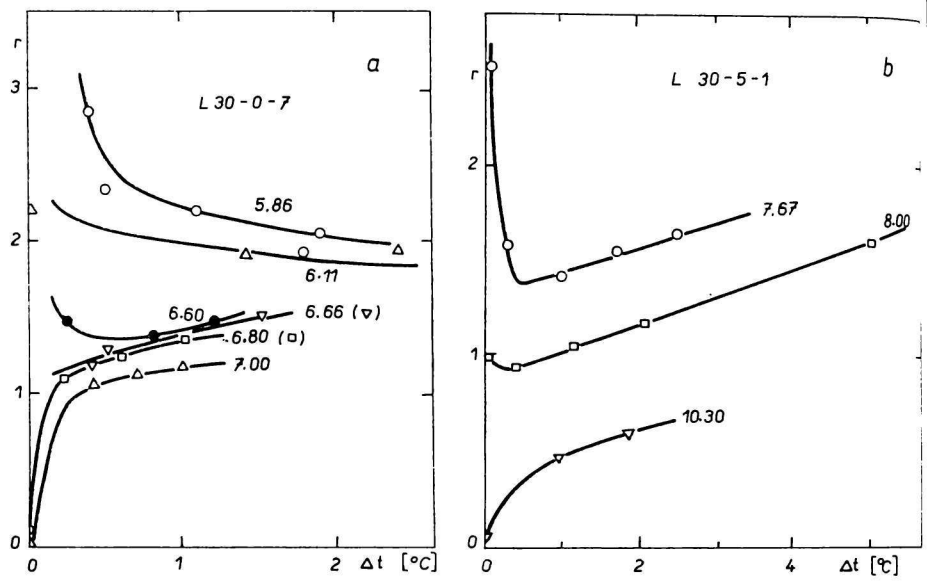


*Fig. 8a, b.* Experimental determination of the critical concentration in the two systems of Fig. 6 (see also Fig. 7).

curve must be known. It can be established by measuring the phase-volume ratio as a function of temperature and concentration. Fig. 7 illustrates this procedure for a binary mixture. According to the lever rule the phase-volume ratio $r$ is given by

$$r = V'/V'' = (\varphi'' - \varphi)/(\varphi - \varphi'),$$

where $V'$ and $V''$ denote the volumes of the dilute and polymer-rich phases and $\varphi'$ and $\varphi''$ their whole polymer volume fractions.

It can be shown [1, 2] that multicomponent systems also exhibit the volume-ratio behaviour illustrated in Fig. 7. Fig. 8 refers to the system polyethylene—diphenyl ether and shows that the phase-volume method yields accurate values of $\varphi_c$. In the example of Fig. 8*a* the critical concentration must evidently lie between 6.6 and 6.8% (w/w).

### *Solvent—polymer 1—polymer 2 systems*

Upon addition of a second polydisperse polymer to the systems discussed so far, the situation becomes considerably more complicated. First of all, with simplified systems, visualization as in Fig. 1 is no longer possible, since binary approximation of the two polymers already calls for a four-dimensional isotherm. From the preceding considerations,

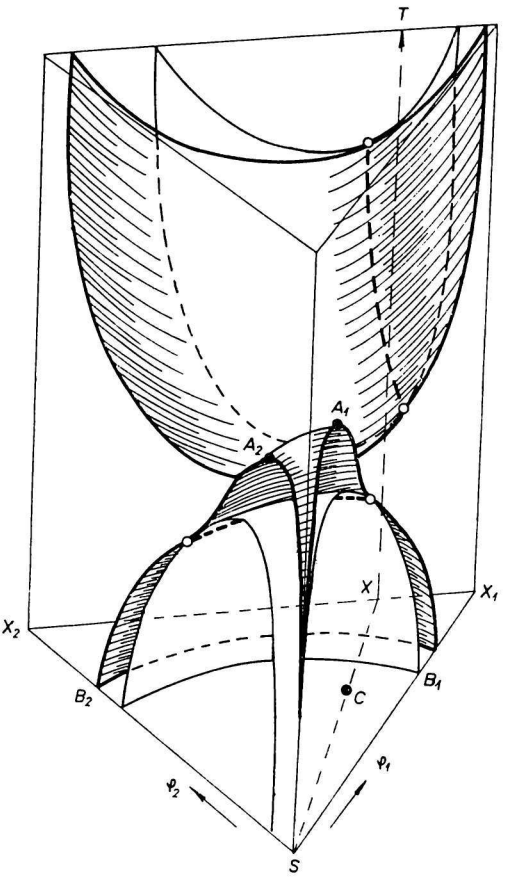


*Fig. 9.* Cloud-point surfaces in a quasi-ternary mixture containing a low-molecular-weight solvent $S$ and two polydisperse polymers ($X_1$ and $X_2$).
——— cloud-point curves;
o – – o critical lines;
——— spinodals.
$A_1$ and $A_2$: quasi-binary precipitation threshold (schematical).

However, we can deduce some features of a three-dimensional quasi-ternary section. Fig. 9 gives a schematical example.

If the two quasi-binary solvent–polymer systems contain miscibility gaps, the two relevant lateral faces of the prism will show all the details noted in the preceding section. Hence, we must expect cloud-point surfaces and coexistence and shadow surfaces to extend into the prism and to connect the corresponding curves in the $TSX_1$ and $TSX_2$ planes. There must be a critical line running along the cloud-point surface and, within the gap, a spinodal surface must be present that touches the cloud-point surface along the critical line.

The miscibility gap may be lacking in one of the two solvent–polymer systems and/or be present in the polymer 1–polymer 2 system. Further, the phenomena described may, or may not go with lower consolute demixing, showing that the liquid–liquid phase relations in quasi-ternary systems may vary considerably and be very complicated.

The two experimental examples shown in Figs. 10 and 11 illustrate the effect of polypropylene on the system polyethylene–diphenyl ether. It appears that the stereoregularity of the polypropylene makes quite a difference as regards the phase behaviour, the second

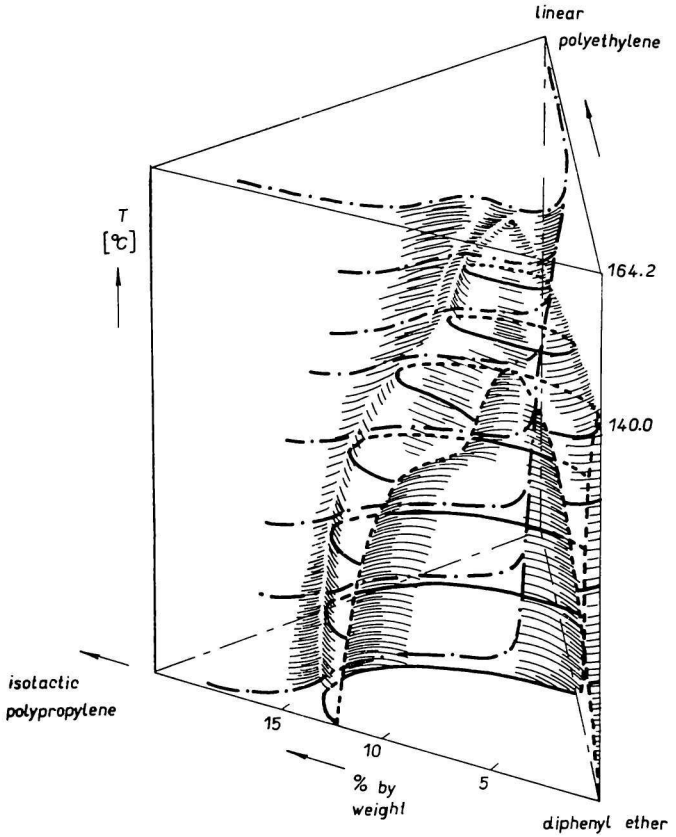


*Fig. 10.* Cloud-point surfaces in the quasi-ternary system diphenyl ether—polyethylene—crystallizable polypropylene.

miscibility gap being absent if the isotactic (crystallizable) polypropylene is replaced by the atactic (non-crystallizing) variety. The second miscibility gap in Fig. 10 was found to be closed at high temperatures [15].

An idea about the cause of this difference can be obtained from a consideration of the spinodal. If the $\Delta G$ function is rewritten so as to account for the second polymer, we have

$$\Delta G/RT = \varphi_0 s_0^{-1} \ln \varphi_0 + \sum \varphi_{1,i}\, m_{1,i}^{-1} \ln \varphi_{1,i} + \sum \varphi_{2,i}\, m_{2,i}^{-1} \ln \varphi_{2,i} + g_{01}\varphi_0\varphi_1 + g_{02}\varphi_0\varphi_2 + g_{12}\varphi_1\varphi_2,$$

where the indices 1 and 2 refer to polymers 1 and 2, and $g_{01}$, $g_{02}$ and $g_{12}$ are the solvent—polymer 1, solvent—polymer 2 and polymer 1—polymer 2 interaction parameters.

Application of condition (*2*) leads to [15]

$$1 + (\varphi_0^{-1} - 2g_{01})\,\varphi_1 m_{w,1} + (\varphi_0^{-1} - 2g_{02})\,\varphi_2 m_{w,2} + [4g_{01}g_{02} - (g_{01} + g_{02} - g_{12})^2 - 2g_{12}\varphi_0^{-1}]\,\varphi_1 m_{w,1}\varphi_2 m_{w,2} = 0.$$

(spinodal)

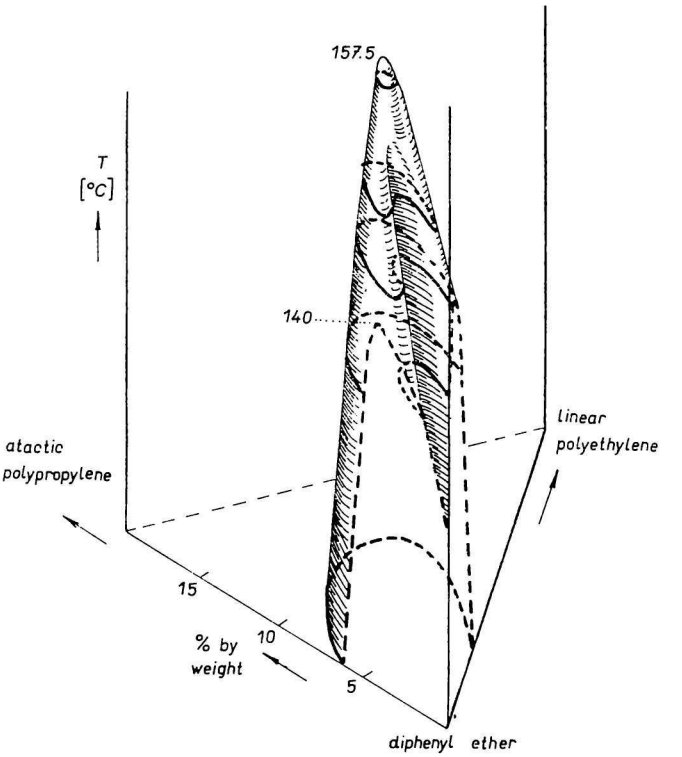


*Fig. 11.* Cloud-point surface in the quasi-ternary system diphenyl ether–polyethylene–non-crystallizable polypropylene.
The polyethylene sample is the same as in Fig. 10.

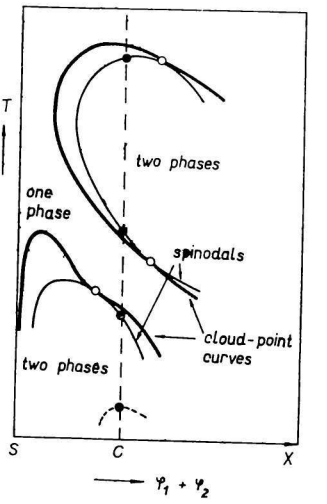


*Fig. 12.* Quasi-ternary section $SXT$ of Fig. 9.
– – – metastable spinodal; ○ critical points.

In the derivation we took $s_0$ equal to 1 and assumed that none of the $g$'s depends on concentration. These limitations do not affect the general validity of the following argument.

If the $g$ parameters should show the usual linear dependence on reciprocal absolute temperature equation (5) would be quadratic in $T^{-1}$. For a given composition, say C in Fig. 9, one could have two spinodal temperatures. A behaviour as displayed by the system in Fig. 10 calls for three intersections in certain composition regions, so that the usual simple $g(T)$ function cannot be appropriate (see Fig. 12). A better approximation includes a linear $T$ term which makes equation (5) bi-quadratic in $T$. In the description of the present system such an extension of the $g(T)$ function is obviously necessary [15].

## *Polymer 1—polymer 2 systems (compatibility)*

The $TX_1X_2$ lateral face of the prism in Fig. 9 relates to the miscibility of two polydisperse polymers differing in chemical structure. This kind of quasi-binary system is of considerable technological importance. Miscibility of two polymers is a rare phenomenon because the entropy of mixing per unit volume is very small (2nd and 3rd terms in equation (5)). Hence, subtle interaction effects may influence the phase behaviour to a considerable degree.

Some idea of the role of interactions and molecular weight distributions can be obtained from Fig. 13, which shows spinodals calculated for various combinations [15]. Depending on the $m_z$ values of the two polymers, the critical point may be nearly anywhere on the

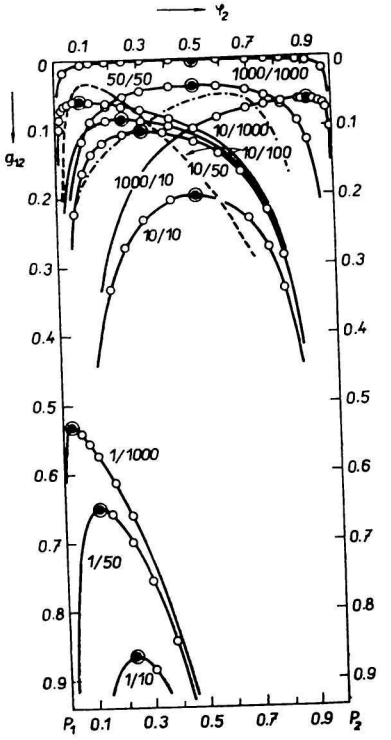


*Fig. 13.* Spinodals (————) and critical points (○) in quasi-binary systems showing the relative locations of the instable regions in mixtures of two polydisperse polymers (upper set of curves) and solutions of a polydisperse polymer in a single low-molecular-weight solvent (lower set of curves). The ratios $m_{w,2}/m_{w,1}$ are indicated.

The two spinodals — — — — and — · — · refer to a concentration dependent $g_{12}$ ($\partial g_{12}/\partial\varphi_2 = -0.1$ and $+0.1$, respectively). The critical points (⊙) at the maxima of the spinodals refer to $a_2/a_1$ values of 1, those on the right-hand branches to $a_2/a_1$ values of 0.5, 0.2, 0.1, 0.05, 0.02, 0.01, 0.001 (from left to right, as far as they are indicated); those on the left-hand branches to $a_2/a_1$ values of 2, 5, 10, 20, 50, 100, 1000 (from right to left); $a_2$ and $a_1$ stand for $m_{z,2}/m_{w,2}$ and $m_{z,1}/m_{w,1}$.

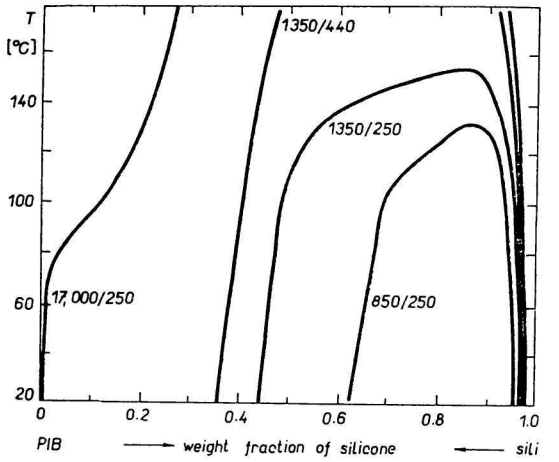


*Fig. 14.* Cloud-point curves of liquid mixtures of silicone (molecular weights 17,000, 1350, 850) and polyisobutene (440, 250). Data from *Allen*, *Gee*, and *Nicholson* [16].

spinodal. Denoting $m_z/m_w$ by $a$, we see that, with $a_1 = a_2$, the critical point will lie at the maximum of the spinodal. In this respect, a polymer mixture resembles a binary system. However, as shown below, this is the only point of analogy. If $a_1/a_2 < 1$, the critical point shifts to $\varphi_2$ values below the maximum of the spinodal and conversely.

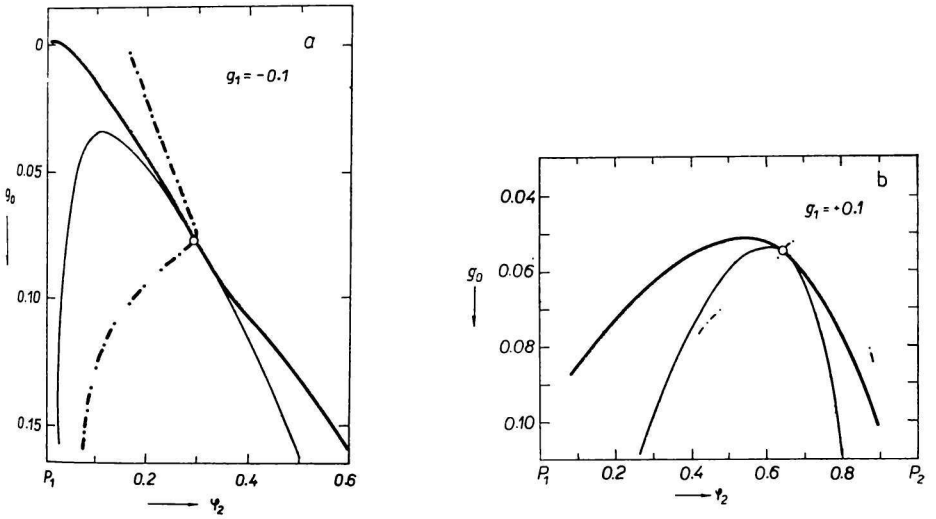


*Fig. 15a, b.* Calculated cloud-point curves (————), spinodals (– – – – –), and shadow curves (— • — • —) for a mixture of two polymers.
$P_1$ = monodisperse: $m_n = m_w = m_z = 10$; $P_2$ = polydisperse: $m_w = 100$; $m_w/m_n = 5$; $m_z/m_w = 7$. Critical points: ○ $g_{12} = g_0 + g_1\varphi_2$.

The locations of spinodals and critical points indicate that the miscibility gap will have the usual asymmetric shape, *i.e.* shift towards the axis of the constituent with the shorter chains. Should the shift be in the opposite direction, this must be due either to

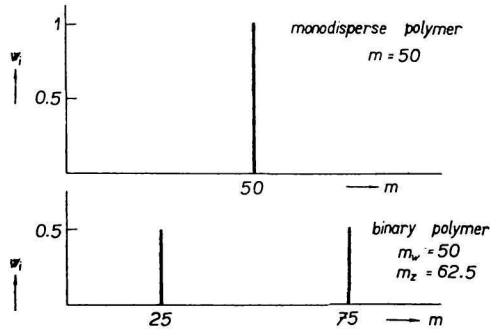


*Fig. 16.* Monodisperse and binary polymers equal in $m_w$.

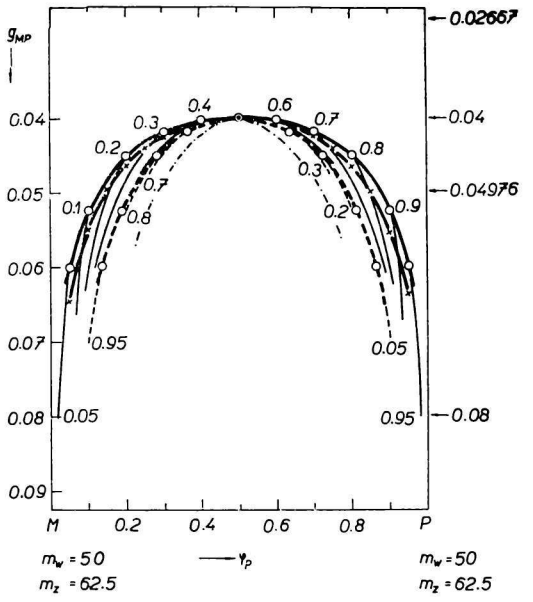


*Fig. 17.* Compatibility of two chemically different polymers with identical distributions. Two binary polymers (see Fig. 16): ———— cloud-point curve; — — — shadow curve; —, – – coexistence curves for various values of $\varphi_P$.
Two monodisperse polymers: —×— cloud-point curve; — • — • — spinodal; ⊙ critical point.

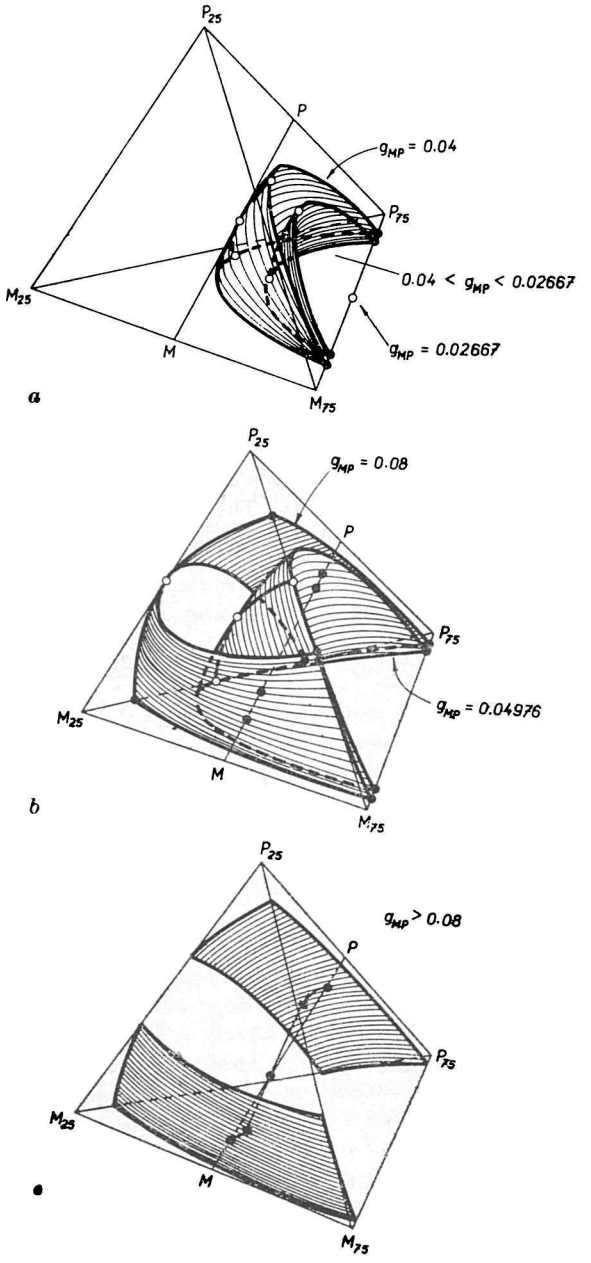


Fig. 18a–c. Isothermal sections showing binodal surfaces referring to the $g_{MP}$ values in Fig. 17.

○ critical points.

Fig. 18c shows the location of a tie line (● —— ●).

a large difference between the two $a$ values or, perhaps more probably, to a concentration dependence of $g_{12}$. Fig. 13 shows two examples for the 10/100 case calculated on the basis of a linear concentration dependence of $g_{12}$. If $\partial g_{12}/\partial \varphi_2 > 0$, the unstable region is shifted towards the $P_2$ axis, *i.e.* towards the axis of the constituent with the larger chains.

This finding may be considered to shed some light on the unexpected locations of cloud-point curves reported by *Allen*, *Gee*, and *Nicholson* [16]. These authors studied mixtures of low-molecular-weight polyisobutenes and silicones and found miscibility gaps shifted towards the silicone axis. The silicones, however, had the longer average chain lengths of the two polymers. Fig. 14 gives the experimental cloud-point curves and Fig. 15 two curves calculated from equation (*1*) with given values of $s_0$. The calculated curves are not quite representative, first of all because in calculations with equation (*1*), polymer 1 is taken to be monodisperse; however, Fig. 15*b* shows the shift towards the $P_2$ axis under the influence of the positive concentration dependence of $g_{12}$, which outweighs the effect of the entropy of mixing here.

Cloud-point curves can also be calculated for two polydisperse polymers. Let us first consider the step from monodisperse to binary polymers and assume the two molecular weight distributions to be identical (see Fig. 16). The cloud point, coexistence and shadow curves for such a symmetrical case are shown in Fig. 17. As to the truly binary 50/50 system, the cloud-point curve (which for this system is identical to the coexistence

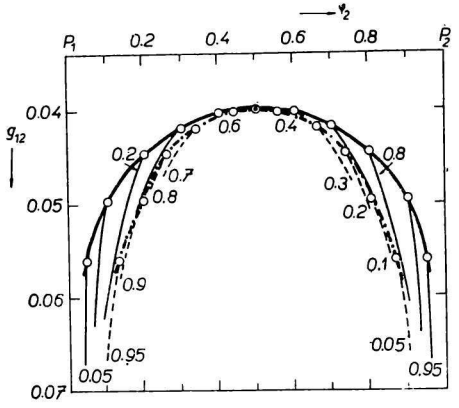


*Fig. 19.* Compatibility of two chemically different polydisperse polymers $P_1$ and $P_2$ with identical exponential distributions ($m_w = 50$; $m_w/m_n = 1.33$; $m_z/m_w = 1.25$).
——— cloud-point curve; — • — • — shadow curve; ——, – – coexistence curves for various values of $\varphi_2$.

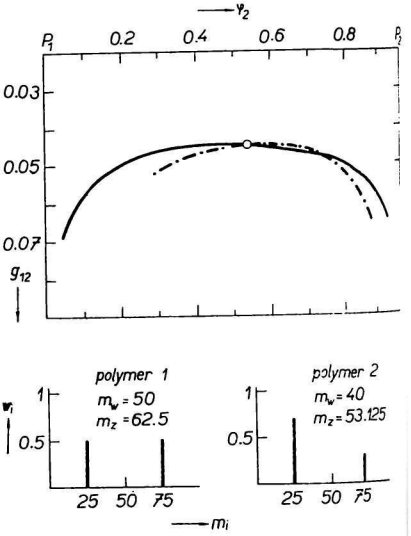


*Fig. 20.* Compatibility of two chemically different binary polymers (distributions shown).
——— cloud-point curve; — • — • shadow curve; o critical point.

curves) will of course be symmetrical, with the critical point located at the maximum.

For the two binary polymers we find the same spinodal as before ($m_{w1} = m_{w2} = m$) and the critical point is located in the maximum of the spinodal ($a_1 = a_2$). We note that the maximum of the cloud-point curve also coincides with the critical point, but the coexistence curves for a given overall concentration $\varphi_p$ are not symmetrical with respect to $\varphi_p = 0.5$. Neither do the shadow and cloud-point curves coincide, the former being located under the latter over the whole composition range.

At first sight, the asymmetry with identical distributions in the two polymers might seem surprising. However, if we consider a three-dimensional isothermal section of the four-dimensional temperature-composition diagram, we see that the symmetry is only partial. From Fig. 18, which is a schematic representation of such isotherms relating to the $g_{12}$ values in Fig. 17, it appears that, in fact, only the $M_{25}P_{25}$ and $M_{75}P_{75}$ axes are symmetrical; the other two ($M_{25}P_{75}$ and $P_{25}M_{75}$) are not. This explains why the diagram in Fig. 17 shows the peculiar features indicative of polydispersity in the constituents.

Similarly as in the preceding discussion in quasi-binary systems, the extension from binary to multicomponent polymers does not disclose any new features. Fig. 19 shows a two-dimensional phase diagram for two identical continuous distributions with the same $m_w$ and $m_z$ values as the two binary polymers in Fig. 17. The only difference is a further widening of the miscibility gap relative to that in the truly binary example.

As soon as the two distributions come to differ to some extent, the asymmetry manifests itself, *i.a.* in the shadow curve, which assumes the location known in polymer solutions, *i.e.* with one branch under and the other one over the cloud-point curve (Fig. 20).

### *Solvent—non solvent—polymer systems*

The most common type of quasi-ternary system is the solvent—precipitant—polymer solution frequently used in polymer fractionation. The simplest case — solvent—non solvent—binary polymer — can be considered with the aid of a three-dimensional isothermal section. Fig. 21 gives an example.

If the influence of temperature in the discussions of quasi-binary systems is replaced by that of non solvent (volume fraction $\varphi_1$) all the peculiarities referred to above are noted also in quasi-ternary systems. Mixtures of the binary polymer $X$ with solvent $S$ and non solvent $NS$ are represented by points in the quasi-ternary section $S-NS-X$. The cloud-point curve $ABC$ is obtained by plotting the $\varphi_1$ value at incipient phase separation *vs.* the whole polymer concentration $\varphi_2$ ($= \varphi_{2,1} + \varphi_{2,2}$). It has a precipitation threshold $B$ which will, as a rule, not coincide with the critical point in section $S-NS-X$. We further note that the cloud-point curve should not be expected to represent coexisting phases and there will be shadow and coexistence curves.

Quasi-ternary sections for polydisperse polymers may be calculated by means of equation (4), in which all $m_{1,i}$ are put equal to 1, so that $\varphi_1$ may be considered to represent the non solvent concentration. In Fig. 22, where $X$ denotes an exponential (Schulz–Zimm) distribution, the polydispersity reveals itself in a similar way as it does in quasi-binary systems. Fig. 23 shows that the critical point travels to larger whole polymer concentrations according as $M_z$ increases at constant $M_w$.

These figures were calculated for a given set of $g$ values. The choice of these markedly affects the location of the miscibility gap, as is borne out by Fig. 24. The two-phase regions will be largest if the solvent is not too good, and the non solvent not too poor.

An interesting quasi-ternary case is a system the two low-molecular-weight components

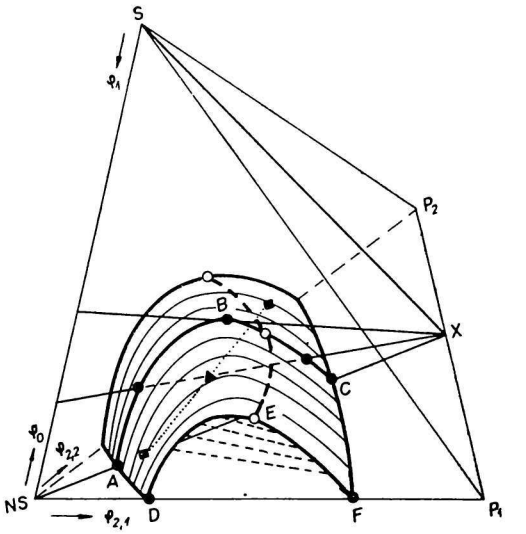


*Fig. 21.* Miscibility gap in a quaternary system containing two macromolecular homologues $P_1$ and $P_2$, a solvent $S$ and a non solvent $NS$. The chain lengths of $P_1$ and $P_2$ differ ($m_2 > m_1$).

Cloud-point curve of polymer mixture $X$: $ABC$; critical line: — o – – o –; tie line for system ▲: ■ ■; tie lines in the truly ternary system $S-NS-P_1$: – – – –.

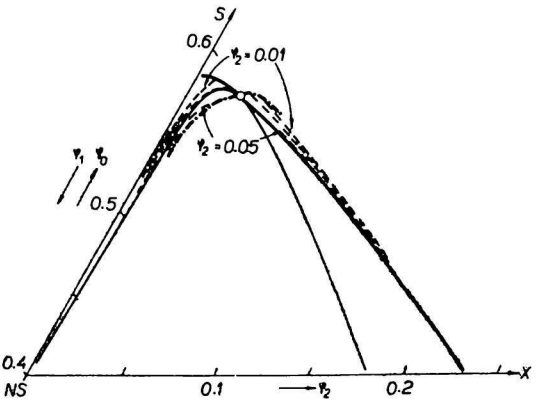


*Fig. 22.* Calculated cloud-point (————), shadow (— • — • —) and coexistence (– – –) curves in a quasi-ternary system for $g_{01} = 0$, $g_{02} = 0$, $g_{12} = 1$. Polymer distribution $X$: exponential, $M_w$: $131.7 \times 10^3$, $M_w/M_n = 2$. Solvent, non solvent and whole polymer concentrations: $\varphi_0$, $\varphi_1$, $\varphi_2$.

o critical point; ———— spinodal.

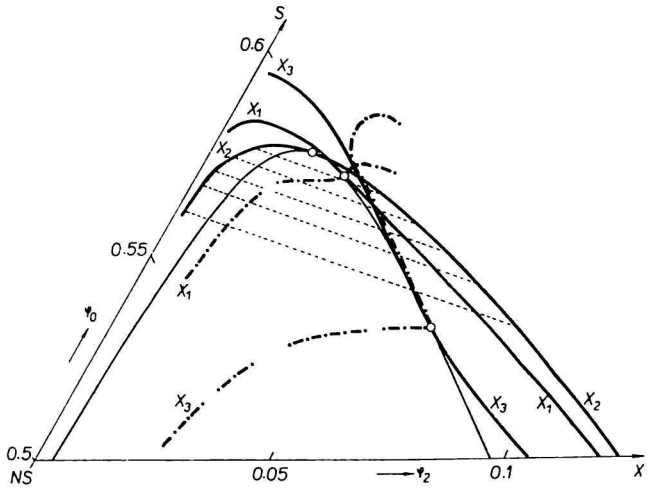


*Fig. 23.* Calculated cloud-point (————) and shadow (—·—·—) curves in quasi-ternary systems for $g_{01} = 0$, $g_{02} = 0$, $g_{12} = 1$. Polymer distributions: $M_w = 131.7 \times 10^3$; $X_1$: $M_w/M_n = 2$. $M_z/M_w = 1.5$; $X_2$: monodisperse; $X_3$: $M_w/M_n = M_z/M_w = 10$. ——— spinodal; — — — tie lines for monodisperse polymer; ○ critical points.

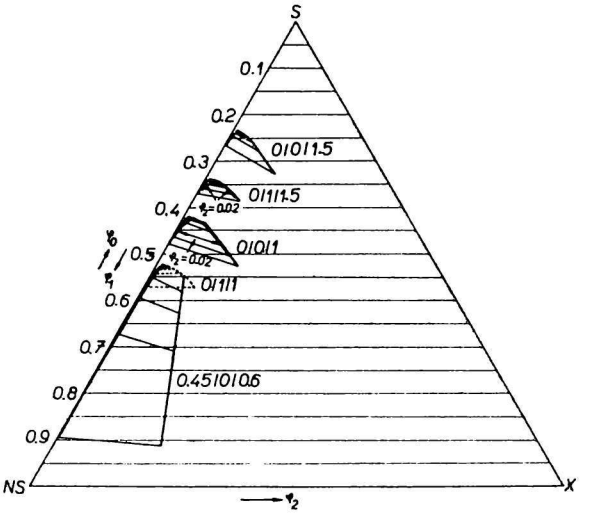


*Fig. 24.* Coexistence curves (— , — —) for an exponential distribution ($M_w = 131.7 \times 10^3$; $M_w/M_n = 2$) for various indicated sets of $g_{02}/g_{01}/g_{12}$ values. ———, — — — tie lines. Whole polymer concentration $\varphi_2 = 0.01$, unless stated otherwise.

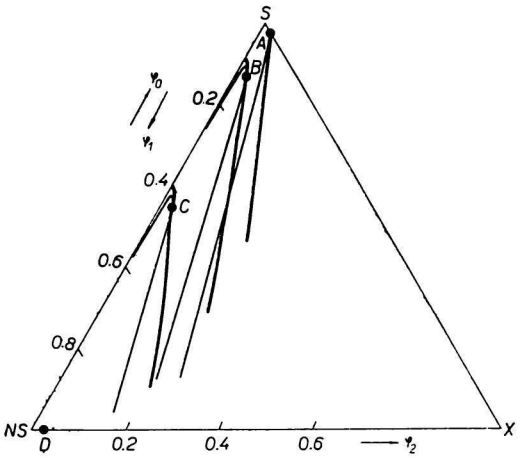


*Fig. 25.* Calculated cloud-point curves (————), spinodals (– – – –) and critical points (●) in a quasi-ternary solvent—non solvent—polydisperse polymer system. *X*: $M_w = 4 \times 10^5$; $M_w/M_n = 2.15$; $M_z/M_w = 2$. Various sets of $g_{02}/g_{01}/g_{12}$ values, *A*: 0.517/0/0.7; *B*: 0.5/0/0.65; *C*: 0.45/0/0.6; *D*: 0.4/0/0.517.

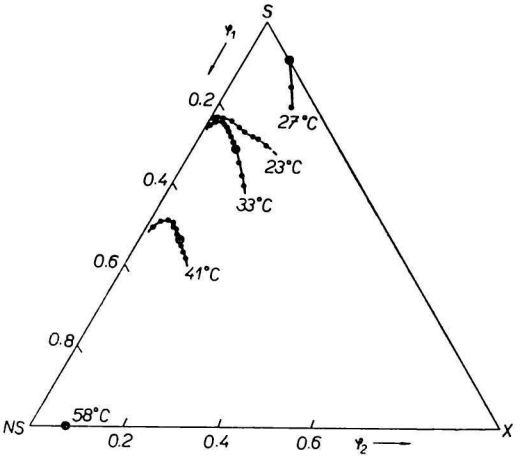


*Fig. 26.* Experimental cloud-point curves (————) in the system cyclohexane (*S*)—ethylcyclohexane (*NS*)—polystyrene (*X*) at various temperatures. ● critical points determined by the phase-volume method.
— — — cloud-point curve in the system benzene (*S*)—methanol (*NS*)—polystyrene (*X*) . *X*: $M_w = 4.1 \times 10^5$; $M_w/M_n = 2.8$; $M_z/M_w = 2.0$.

which are both $\Theta$ solvents, while its temperature is intermediate between the two $\Theta$ points. One might look upon Fig. 25 as an example of such a system. The distribution $X$ was so chosen as to roughly conform to a sample of polystyrene with which cloud-point measurements were performed in mixtures of cyclohexane and ethylcyclohexane. The

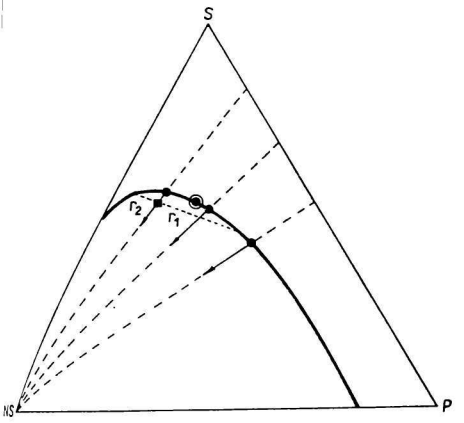


*Fig. 27.* Schematical ternary phase diagram for a solvent—non solvent—monodisperse polymer system. The phase-volume ratio $r$ is given by $r_1/r_2$. ⊙ critical point.

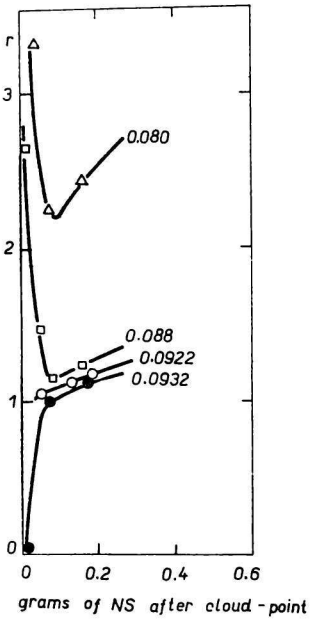


*Fig. 28.* Experimental phase-volume ratio $r$ for various values of the volume fraction of the whole polymer at the cloud point. System: cyclohexane ($S$)—ethylcyclohexane ($NS$)—polystyrene at 33°C (see Fig. 26).

results in Fig. 26 show that one actually finds the gradual shift of the cloud-point curve predicted by Fig. 25. It further shows that a cloud-point curve may exhibit a depression (benzene—methanol) as suggested by some of the calculated examples.

The location of critical points can be established in a similar way as in quasi-binary systems. Measurement of the phase-volume ratio as a function of the amount of non solvent added beyond the cloud point yields a similar kind of relationship. Fig. 27 illustrates this; Fig. 28 gives an experimental example.

## *Polymer fractionation*

Fractionation of polymers with respect to chain length by liquid—liquid separation has always received much attention in polymer science. We may restrict ourselves therefore to referring to the comprehensive reviews [17—21] that have appeared on this subject, and only add a few marginal notes relevant to the present context.

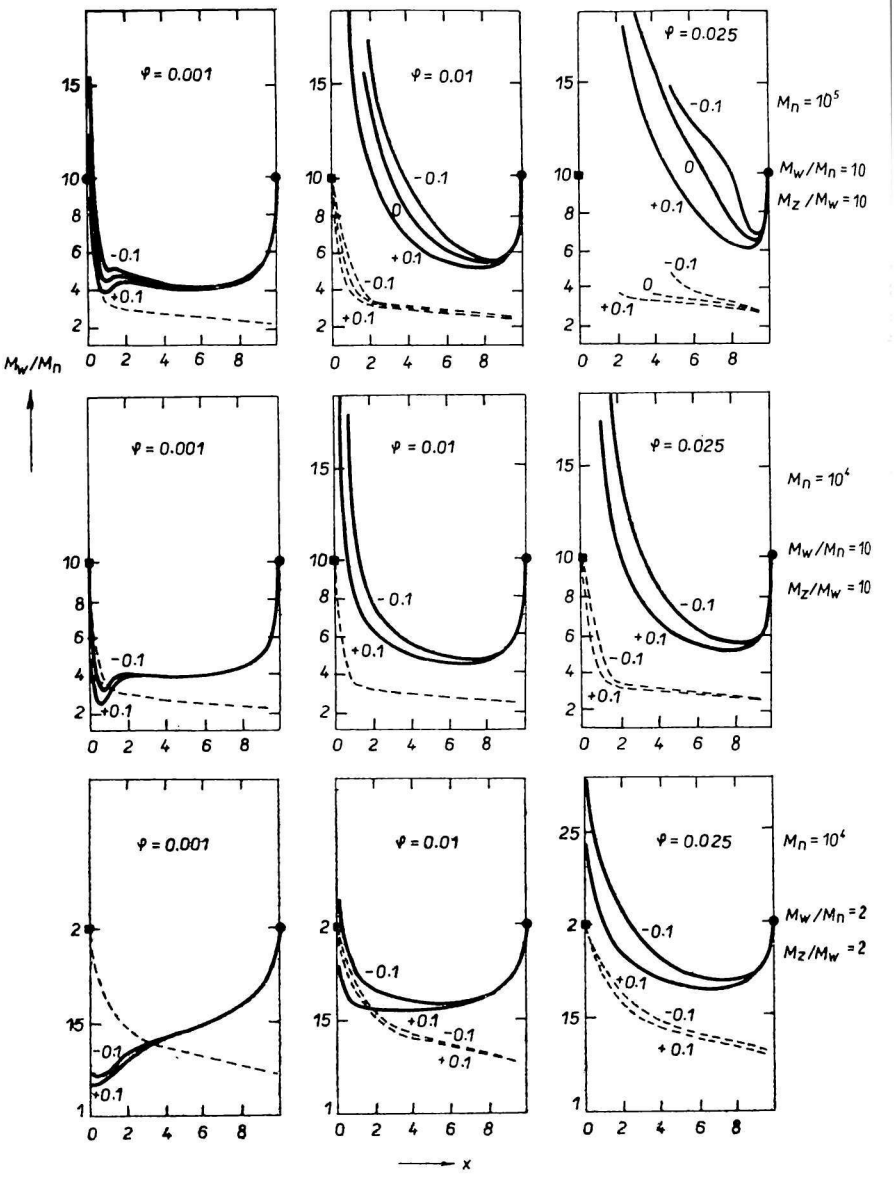


*Fig. 29.* Fractionation efficiency, expressed as $M_w/M_n$ of the fraction *vs.* fraction size for various values of the overall polymer concentration $\varphi$.
—— fraction in concentrated phase; — — — fraction in dilute phase. The abscissa shows $x$, the relative size of the fraction in the concentrated phase.
The interaction parameter is given by $g = g_0 + g_1\varphi$; values of $g_1$ are indicated. Characteristics of the initial distributions are given on the right.

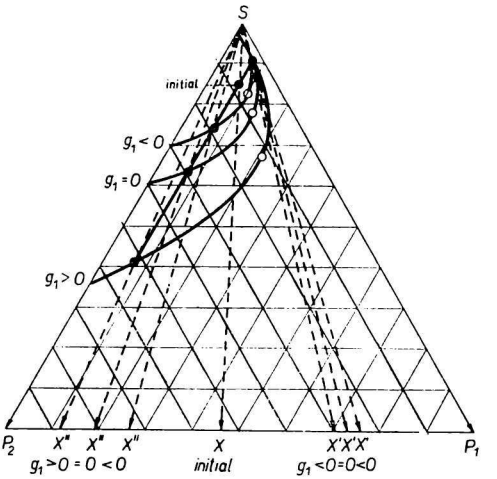


*Fig. 30.* Influence of the extension of the miscibility gap on fractionation efficiency. The interaction parameter depends on concentration: $g = g_0 + g_1\varphi$.

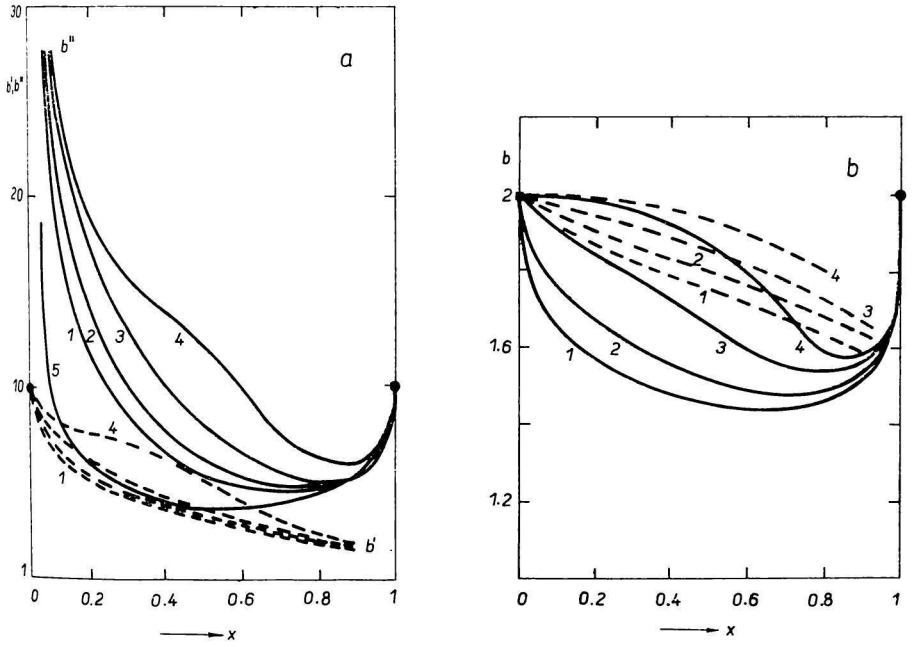


*Fig. 31a, b.* Fractionation efficiency calculated for two initial distributions and various sets of the interaction parameters $g_{02}/g_{01}/g_{12}$.

Drawn curves: polymer-rich phase, dashed curves: dilute phase ($b = M_w/M_n$), $x$ is the relative size of the fraction in the concentrated phase. *a)* $g_{02}$-$g_{01}$-$g_{12}$.

*1.* 0-1.2-1; *2.* 0-1.4-1; *3.* 0-1.6-1; *4.* 0-1.8-1; *5.* 0.45-0-0.6 (also quasi-binary); $\varphi = 0.01$.

*b)* $g_{02}$-$g_{01}$-$g_{12}$. *1.* 0.45-0-0.6; *2.* 0-0-1; *3.* 0-1-1; *4.* 0-1.4-1; $\varphi = 0.01$.

The efficiency of a preparative fractionation depends on a number of experimental conditions such as whole polymer concentration, fraction size, *etc.* [22]. As to quasi-binary systems, in which phase separation is brought about by a change in temperature, calculation shows that preference should be given to such systems in which the interaction parameter increases with the polymer concentration. Fig. 29 illustrates this for a $g(\varphi)$ function of the form: $g = g_0 + g_1\varphi$. These findings are in agreement with those reported in Dr. Kamide's contribution to the present Meeting. The cause of this phenomenon is to be sought in the extension of the miscibility gap, which depends on the $g(\varphi)$ relation. Fig. 30 gives a schematical example.

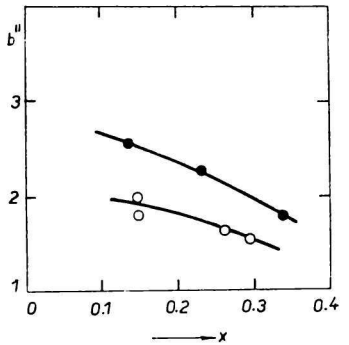


*Fig. 32.* Fractionation efficiency in two quasi-ternary polystyrene systems. Fraction in concentrated phase, $b'' = M_w/M_n$ of the fraction (see Fig. 31).
● benzene—methanol (24°C); ○ cyclohexane—ethylcyclohexane (33°C).

Under comparable conditions (at $g_0$ values where $\varphi$ and fraction size $x$ are equal) we find that the miscibility gap is wider with $g_1 > 0$ than with $g_1 = 0$, and narrower with $g_1 < 0$. This means that the fraction in the concentrated phase $X''$ will be nearest to the pure component $P_2$ if $g_1 > 0$. The widest gap goes with the longer tie lines, meaning that the compositions of the phases differ more according as $g_1$ is larger. It is obvious that this effect favours the fractionation efficiency.

A similar aspect can be noted in quasi-ternary fractionation diagrams. Fig. 31 gives two calculated examples which indicate that a solvent—non solvent pair which itself is near to demixing ($g_{01}$ large) is very unfavourable, whereas the best result is obtained with a non solvent of not too poor and a solvent of not too good dissolving power. Judged from Fig. 24 one would conclude that this behaviour again goes with the extension of the miscibility gap. For qualitative experimental evidence see Fig. 32.

## Conclusions

The polydispersity existing, as is well known, in virtually all polymers, should not be neglected in studies on liquid—liquid phase relationships in systems containing macromolecular constituents. It manifests itself in several ways and distinctly influences the quantitative interpretation of phase equilibria. Fortunately, its influence can readily be accounted for since it appears only in the form of some average molecular weights in important conditions such as consolute state and stability limits.

*Acknowledgements. Thanks are due to Messrs. L. A. Kleintjens, P. H. Hermans, and J. G. M. Creusen for their valuable assistance in the preparation of the manuscript.*

## References


1. Koningsveld R., Staverman A. J., *J. Polym. Sci. A-2*, **6**, 305, 325, 349 (1968); *Kolloid-Z.* and *Z. Polym.* ***218***, 114 (1967).
2. Koningsveld R., *Advan. Colloid Interface Sci.* **2**, 151 (1968).
3. Tompa H., *Trans. Faraday Soc.* ***45***, 1142 (1949).
4. Tompa H., *Polymer Solutions*. Butterworths, London, 1956.
5. Tompa H., *Trans. Faraday Soc.* ***46***, 970 (1950).
6. Gordon M., Chermin H. A. G., Koningsveld R., *Macromolecules* **2**, 207 (1969).
7. Schreinemakers F. A. H., in H. W. Bakhuis Roozeboom: *Die heterogenen Gleichgewichte vom Standpunkte der Phasenlehre*, Vol. III, Part 2. Vieweg, Braunschweig, 1913.
8. Flory P. J., *Principles of Polymer Chemistry*. Cornell University Press, Ithaca, 1953.
9. Huggins M. L., *Physical Chemistry of High Polymers*. J. Wiley, New York, 1958.
10. Rehage G., Möller D., Ernst O., *Makromol. Chem.* ***88***, 232 (1965).
11. Rehage G., Möller D., *J. Polym. Sci. C*, ***16***, 1787 (1967).
12. Gibbs J. W., *Collected Works*, Vol. I, p. 132. Dover Publications Reprint, New York, 1961.
13. Šolc K., *Macromolecules* **3**, 665 (1970).
14. Koningsveld R., Kleintjens L. A., Shultz A. R., *J. Polym. Sci. A-2*, **8**, 1261 (1970).
15. Koningsveld R., Chermin H. A. G., Gordon M., *Proc. Roy. Soc.* (London) ***A319***, 331 (1970).
16. Allen G., Gee G., Nicholson J. P., *Polymer* **2**, 8 (1961).
17. Cragg L. H., Hammerslag H., *Chem. Rev.* ***39***, 79 (1946).
18. Desreux V., Oth A., *Chem. Weekbl.* ***48***, 247 (1952).
19. Guzman G. M., in J. C. Robb and F. W. Peaker: *Progress in High Polymers*, Vol. I, p. 113. Heywood, London, 1961.
20. Cantow M. J. R., *Polymer Fractionation*. Academic Press, New York, 1967.
21. *Proceedings 3rd Microsymposium 'Distribution Analysis and Fractionation of Polymers'*, Prague, 1968.
22. Koningsveld R., *Advan. Polym. Sci.* **7**, 1 (1970).